2021 年臺灣國際科學展覽會
優勝作品專輯

作品編號 **080020**

參展科別 生物化學

作品名稱 **An In-Depth Patch-Clamp Study of HCN2 Channel (Year II): Discovery of Novel Biomarkers and Therapy for Ih Current Suppression in Autism Spectrum Disorders**

得獎獎項 大會獎 一等獎

國　　家 **United States**

就讀學校 **Maggie L Walker Governor's School for Government and International Studies**

指導教師 **Sharon B Snyder**

作者姓名 **Perisa Satish Ashar**

關鍵詞 **Ih current、sedation、Autism**

作者照片


PERISA
FINALIST
Selen Qarajeh
Astha Ray
Roberto Rodriguez
Michaela Samanta
Zachary Schneider
Andy Shar
Cameron
Anna Skierska
Peter
Gabriel
Rojas Lara
Schorowsky

Overview

The main goal of this study was to address a variety of topics concerning the role of the Ih current in HCN channels of SHANK Wild-Type and Knock-Out Thalamus Neurons (as described further below). This research explored the cellular effects of sedation (like Dexmedetomidine) and laser light stimulations on the Ih current of neurons, as well as discovering novel biomarkers for detecting Autism Spectrum Disorder. This study also showed that methods (like utilizing laser therapy with and without various photosensitizers) have the potential in raising depressed Ih currents of SHANK Knock-Out neurons.

Introduction

Autism spectrum disorder (ASD) is a developmental disorder that affects communication and behavior. Not only does ASD have a major impact on the development and social integration of affected individuals, but it is also the most heritable of all psychiatric disorders. Postmortem examination of ASD brains have shown disorganized gray and white matter, increased number of neurons, decreased volume of neuronal soma, and increased neuropil (Varghese et al., 2017)., Mutations in SHANK family genes have been associated with syndromic and idiopathic ASD, in addition to other neuropsychiatric and neurodevelopmental disorders (like schizophrenia). In mice, mutations in the genes encoding SHANK1, SHANK2, and SHANK3 often result in marked behavioral phenotypes, including an increase in repetitive routines, altered social behavior, and anxiety-like phenotypes, which are very similar to the symptoms described in some human neuropsychiatric disorders (Monteiro and Feng, 2017). There are different variations in SHANK mutations. In this study, SHANK 688 mice (otherwise known as *Shank3*$^{\Delta 13–16}$ knockout mice) were studied, which lacked exons 13-16. These mice have shown a significant decreased social motivation and synaptic physiology. However, the protein structure as well as thalamus neuron electrophysiological properties of these mice have never been studied (Peça et al., 2011). While behavioral differences have been noted, finding differing cellular mechanisms (like the Ih current patterns) could enable us to find out how and why certain patients suffer from specific symptoms of ASD.

Sedation is also very important in biology and chemistry. Sedatives are medicines taken for their calming and soporific effects, due to their abilities to lower a person's awareness and responsiveness to their environment (Lingappan, 2017). Dexmedetomidine (DEX) is a sterile sedative and is delivered as an intravenous (IV) anesthetic to patients. It is an alpha2 adrenoceptor agonist, as it selectively stimulates alpha adrenergic receptors. Alpha2 adrenoceptors are a kind of G protein-coupled receptors (family of receptors that activate cellular responses). Alpha2 has three homologous subtypes: Alpha2A, Alpha2B, and Alpha2C. In the experiment, the Alpha2C subtype was studied in the thalamus region of the brain. Additionally, the effect of Dexmedtomidine have never been studied on SHANK WT and SHANK KO thalamus neurons in *Mus Musculus*.

The HCN (hyperpolarization-activated cyclic nucleotide-gated) channels are a type of pore-loop cation channels (Robinson, 2002). These channels open or become activated when the membrane potential is hyperpolarized (Emily, 2015). HCN channels are involved in controlling neuronal excitability, synaptic transmission, and rhythmic oscillatory activity in neurons and their networks. The cation current that runs through HCN channels is called the Ih current (Benarroch, 2013), which is activated when the membrane potential is between -50 to -60mV.

Previous studies have shown that the Ih current affects the excitability of primary sensory neurons in rats (Hogan, 2008). The current Ih current has a vital role in controlling cardiac and neuronal rhythmicity. If the Ih current is lacking, there will be behavioral defects and changed dopamine levels (Gonzalo-Gomez, 2012).

Cyclic Adenosine Monophosphate (cAMP) is a derivative of ATP (adenosine triphosphate). It is a second messenger that is utilized for intracellular transduction. cAMP is involved with activating protein kinases. cAMP has a chemical formula of $C_{10}H_{11}N_5O_6$ and a molar mass of 329.206 g/mol. It binds to and regulates the function of other cyclic nucleotide-binding proteins such as the Rap guanine nucleotide exchange factor 2. In eukaryotic cells, cAMP regulates glycogen, sugar, and lipid metabolism. Several cyclic nucleotides, especially cyclic adenosine monophosphate (cAMP), facilitate the activation of the HCN channel, potentially leading to a higher Ih current. The binding of cAMP lowers the threshold potential of HCN channels. As a result, this causes the activation of HCN channels (Bois et al., 2011). Other studies have also discovered that through the patch-clamp fluorometry technique that fluorescent cAMP analogs fluoresce strongly in the hydrophobic binding pocket and exerts regulatory effects on HCN channels similar to those imposed by cAMP (Wu et al., 2011).

Fluorescein isothiocyanate (FITC) is a derivative of fluorescein used in wide-ranging applications. FITC has excitation and emission peak wavelengths of about 495-515nm, which is ultimately a green color ("FITC"). Due to is stability and efficiency, FITC is the most used fluorescence labelling reagent (Chaganti et al., 2018). However, no studies have been done on the direct interactions and mechanism changes between FITC and the HCN channel. F002 is a compound in which FITC is covalently bonded/conjugated with cAMP. There has not been a study of F002 on the HCN Channel and Ih Current.

Laser surgeries are frequently used to treat certain parts of the body (like removing tumors or preventing blood loss, treating skin conditions, and fixing eye problems (myopia, hyperopia, astigmatism). However, the effect of laser light on the Ih Current has never been studied. Laser with various photosensitizers and messenger compounds (like cAMP, FITC, and F002) may hold a promising future in acting as novel therapies for SHANK KO mice (and thus individuals with Autism Spectrum Disorder) as well as therapies for improving cognitive behavior after a patient undergoes major sedation.

DEX's effect on the Ih current has also never been studied in thalamus neurons. The purpose of this study is to investigate the effect of DEX (with and without compound cAMP) as well as laser light stimulation (with and without cAMP, FITC, FITC+cAMP, and F002) on Ih currents in WT and KO mice. The research questions for this project were: "Can Dexmedetomidine lower the Ih Current Amplitude of the HCN Channel in SHANK Knockout and Wild-Type thalamus neurons of *Mus Musculus*? Can cyclic AMP mitigate the reduction of the Ih current (if caused by DEX)? Can there be certain electrophysiological biomarkers that can differentiate Knock-Out Mice from Wild-Type mice (such as observing the positive un-normalized Ih current amplitude)? Will lasers (with and without additional compounds and photosensitizers including cAMP and FITC) activate the HCN channel, increase the Ih current amplitude, and perhaps be considered as moderate treatments for the suppression of Ih currents (especially if noted in Knock-Out mice)? The hypotheses were: If Dexmedetomidine is used on the HCN Channel in Mus Musculus, then the Ih current amplitude will be lowered. This hypothesis is supported by Chen's research, who found out that DEX lowers neuronal delayed-rectifier Sodium and Calcium Currents (Chen, 2009). If cyclic AMP is used on the HCN2 Channel (before DEX) in Mus Musculus, then it will minimize the reduction of the Ih current (if

caused by DEX). If a SHANK 688 KO mice is studied, then it will have a suppression in positive, un-normalized Ih currents (compared to its corresponding SHANK Wild Type mouse). If lasers (with various photosensitizers) are studied on SHANK 688 KO mice, then they will reverse the suppression of the Ih current by activating the HCN channel.

Methods and Materials

This project was divided into four parts. Part 1A studied the effects of DEX on thalamus neurons of WT mice. In Part 1A, prior to the experiment, 7-8 day old mice were genotyped. Before patch-clamping, mice had already been deceased. A 1L sucrose-ACSF solution (artificial cerebrospinal fluid) was made comprising of (in mM): 240 sucrose, 2.5 KCl, 1.25 NaH_2PO_4, 0.5 $CaCl_2$, 3.5 $MgCl_2$, 25 $NaHCO_3$, 0.4 ascorbic acid and 2 sodium pyruvate. The pH of the sucrose solution (and Krebs 1X solution) was maintained between 7-7.5, and its osmolarity (by an Osmette A machine) was 290-300 osmoles of solutes per liter of solution. The sucrose solution was at -80 °C for only 20 minutes. The 2L 1x standard Krebs ACSF solution (an artificial cerebrospinal fluid) was made of (in mM): 124 NaCl, 3.6 KCl, 1.2 NaH_2PO_4, 2.5 $CaCl_2$, 1.2 $MgCl_2$, 25 $NaHCO_3$, 11 glucose, 0.4 ascorbic acid and 2 sodium pyruvate. Two 2x2cm squares of agarose solution were cut. Tube lines will send oxygen (O_2) to the sucrose solution. About 15ml of the sucrose solution was placed inside a needle, via syringe, which perfused the left heart of the mouse. The mouse (under IsoThesia sedative) was dissected and its brain taken out. The front portion and back portion slices were cut and thrown out.

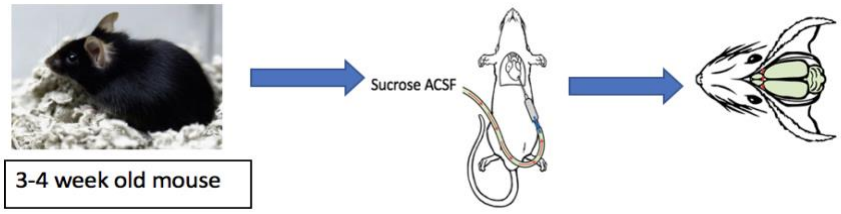

Figure: Diagram of obtaining brain from mouse after trans cardiac perfusion with Scurose ACSF.

The brain was placed (between agarose squares) on top of ice for 10 min. Each of the slices was cut again in the "Camden Techni Edge" tissue splicer machine. The rest of the sucrose solution (contained in a beaker) was placed in ice for 10 minutes, and then placed inside a small tray of the tissue splicer tissue machine. After 5 tissue splices had been finished, they were placed in the container containing Krebs 1x solution at 32°F. The following blockers were added to the standard Krebs ACSF solution in order to isolate Ih currents for this study: 1 mm $BaCl_2$, 1 mm 4-AP, 0.1 mm $NiCl_2$ and 1 μm TTX (Tetrotodoxin). DEX was stored at -80°C, and the DEX 50 nanomolar (nM) mixed solution was made by mixing it with 55ml of the standard Krebs ACSF solution (mixed with the other blockers). One neuron slice was placed on the stage of a 1000x microscope. The Krebs ACSF blocker solution and DEX mixed solutions (which all had tube lines connecting to the micropipette on the tray containing the neuron slice) were placed in separate containers. A NIKON micro-camera showed the image of the neurons (part of the thalamus region) on the first computer. A controller was connected to a micropipette, which had been placed on the slice. A syringe contained the internal solution(also referred to as just K+ solution), comprising of (in mM): 130 potassium gluconate, 5 KCl, 10 phosphocreatine, 10 HEPES, 0.5 EGTA, 2 Na_2-ATP, 0.3 Na-GTP and 2 $MgSO_4$, and was connected to the micropipette by a tube line (as the HCN2 channels are permeable to potassium solutions). By

moving the various functions of the controller, the micropipette was moved in those directions respectively. On a second computer, the "WinWCP" program was opened, which recorded test values for several protocols. While looking for a compatible neuron, the voltage was maintained at -60mV which is about resting voltage of the cell membrane.

Once the micropipette made contact with the cell membrane, more suction was applied to rupture the membrane patch (while still ensuring that the cell membrane was intact). Once the resistance reached at least 100 MOhms, the micropipette offset and the capacity of the cell membrane at a series resistance (the capacity of the cell membrane was measured in pF and the resistance [supplied by the ion channels acting as resistors] was measured in mΩ) were recorded, and suction was applied to form a good seal on the cell. The voltage (VC) clamp (which measured current amplitude) was switched to the IC sensor (which measured voltage). The current was set at 0pA, so that the resting membrane potential was recorded. A "sag+rebound" protocol was selected to test if it is a reticular (RTN) or ventrobasal (VB) neuron by measuring the voltage patterns.

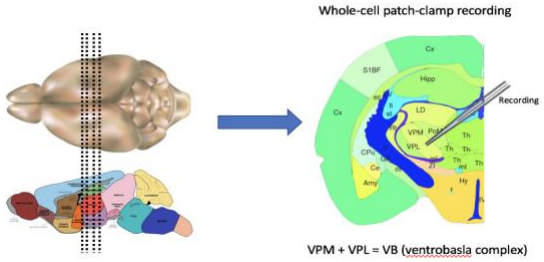

Figure: Schematic of section of the brain utilized (ventrobasal complex) when performing patch-clamping procedures.

The IC was switched again to the VC, and the "Wei_Ih-40mV_100mV_100" protocol was used to measure the effect of the Krebs ACSF block perfusion and DEX mixed solutions on the Ih current amplitude of the two HCN2 channels at the set voltage of -100mV. During the first 20 steps of this protocol, the Krebs ACSF block perfusion solution had an opened passageway to the micropipette. (Each step had a time duration of 32 seconds.) During the next steps, the combination of DEX and the Krebs ACSF block perfusion solutions were opened to the micropipette. The effect of all these solutions was measured on the Ih current amplitude (pA). The values of the Ih current amplitude were reorganized and normalized by dividing that particular Ih current (numerator) by the average of the absolute values of the last electric current of the Krebs ACSF block perfusion solution to the first electric current with the combination of DEX+Krebs ACSF (denominator), and units are not given.

Part 1B studied the cAMP molecule in conjunction with DEX on the Ih current on SHANK WT neurons. The syringe (containing internal solution) now contained an additional 200uM of cAMP, and was connected via tube line to the micropipette. Parts 2A and 2B studied the effects of DEX (with and without cAMP) respectively on SHANK KO mice (lacking exons 13-16). Part 3 compared positive un-normalized, positive Ih current amplitude differences between WT and SHANK KO mice (where electrophysiological biomarkers for ASD could be identified). Part 4 studied the effects of laser light stimulation (in which laser pulses were performed every 6 seconds) with and without specific photosensitizers (K+ (as described in 1A, cAMP, FITC, F002) on the Ih current only in KO mice. Since mice were dealt with in this lab, gloves were worn at all times, and an adult supervisor was always nearby.

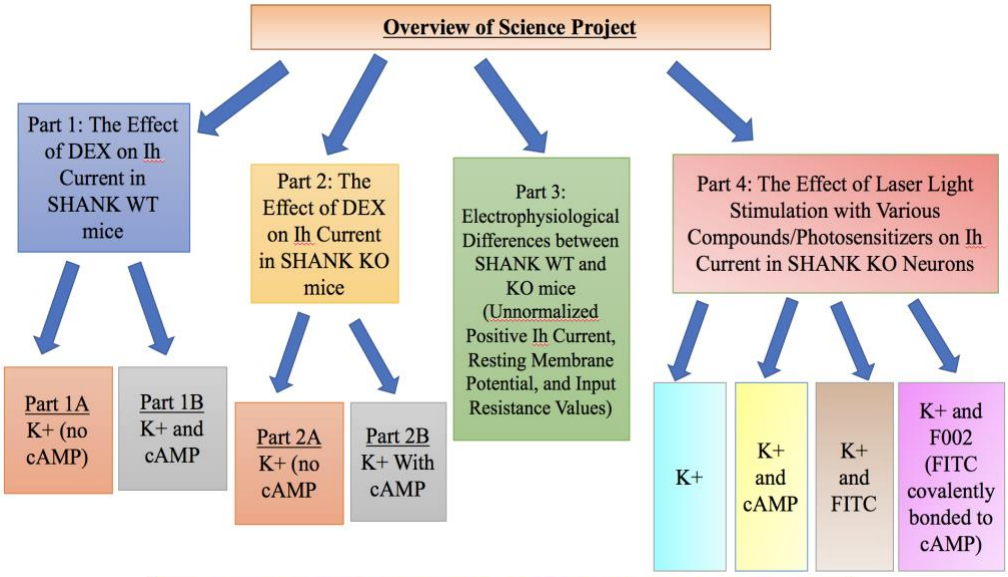

Experimental Outline: The Effect of DEX and Laser Light Stimulation Pulses on the Ih Current of the HCN Channel in Mice Neurons	
Independent Variable	DEX (or Laser Light Stimulation)
Control	Krebs ACSF Block Solution
Dependent Variable	Ih Current Amplitude in Mice
Constants	Genus a species of mice, brand of DEX solution, brand of Krebs ACSF solution,
Number of Trials	7-10

Results

Part 1

An F-Test was done for all of the individual trials to determine if the raw data between the control group and experimental group had equal or unequal variances. A subsequent two-tailed t-test (based on the variance results of the previous F-test) was used to test if the data between the control group (Krebs ACSF) and the experimental group (DEX+ACSF or laser+ACSF) was statistically-significant or not. (The "ACSF Wash Group" was not included in any statistical tests.) Per the bar graphs, DEX lowered the Ih current, while cAMP was able to reduce the depression of the current. Laser pulses were able to activate the Ih current with K+, cAMP, and FITC photosensitizers except F002.

Figure 1

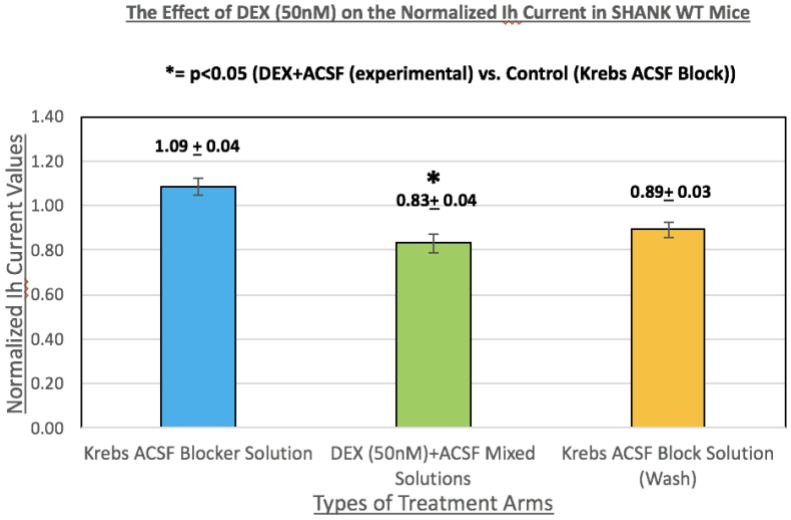

Figure 2

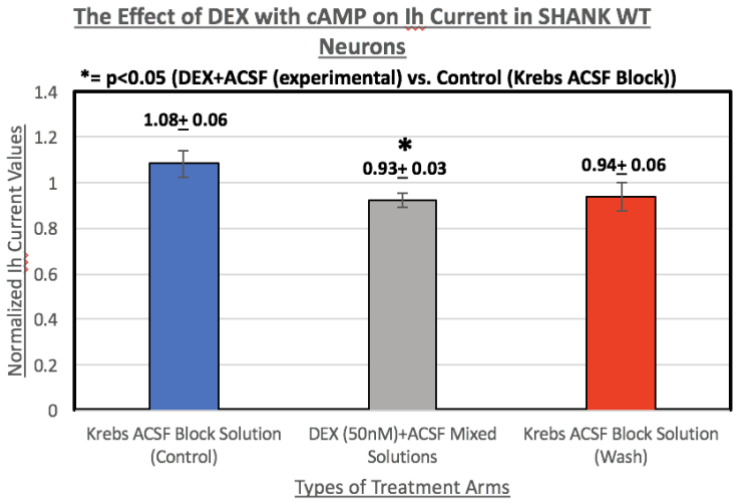

Figure 3

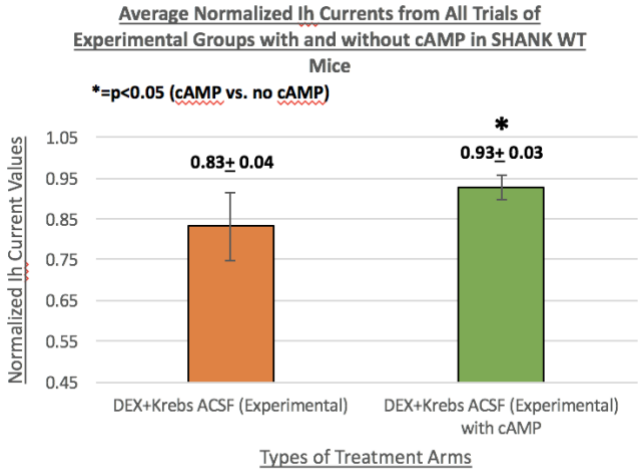

In SHANK 688 Wild-Type neurons, the mean normalized Ih Current of the experimental group (DEX+ACSF) was always lower than the control group (Krebs ACSF). Raw data of the individual trials showed that the line of the normalized Ih current would "drop" in the presence of the experimental group. All of the raw data trials showed that the reduction of the Ih current (caused by the 50nM DEX mixed solution) was statistically significant compared to Krebs ACSF (using two-tailed T-tests), except for Trial #4 (p=0.135). (Note that the Krebs ACSF "wash" group was excluded from statistical testing.) The p-value (measuring the means of Ih normalized currents) of the experimental group (DEX+ACSF) vs. the control group (Krebs ACSF) without cAMP was 6.08 x 10^{-5}. Even with cAMP, the DEX+ACSF experimental group was still lower than the control group. However, cAMP was significant in reducing the depression of the Ih Current caused by DEX. The p-value (measuring the means of Ih normalized currents) of the experimental group (DEX+ACSF) without cAMP vs. the experimental group (DEX+ACSF) with cAMP was 0.00676.

Part 2

Figure 4

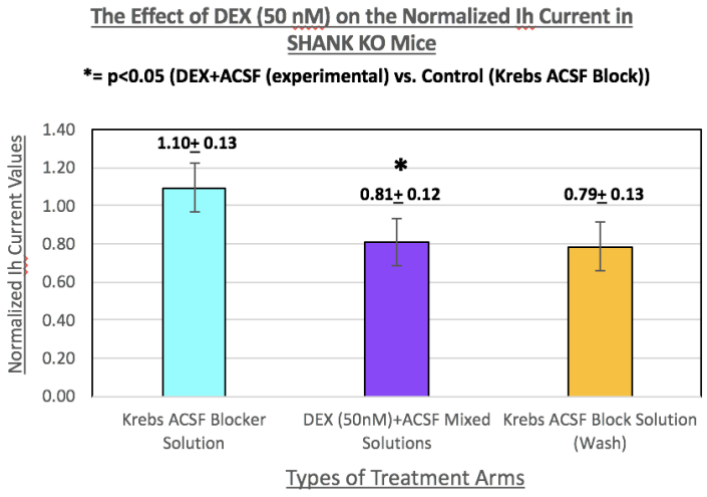

Figure 5

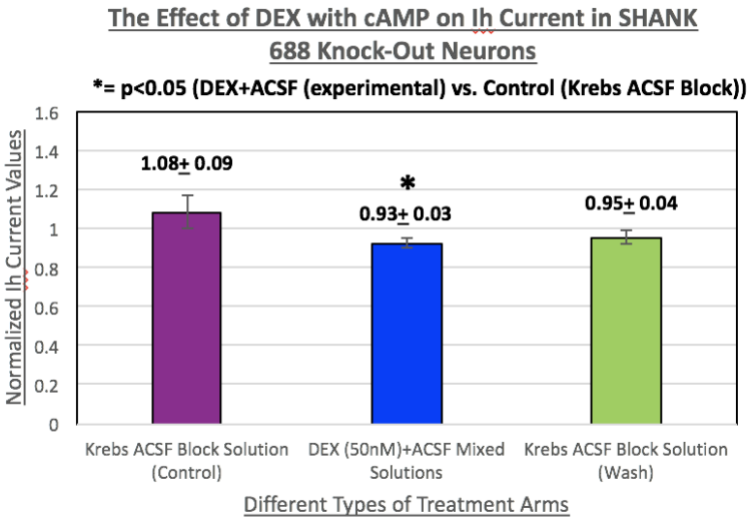

Figure 6

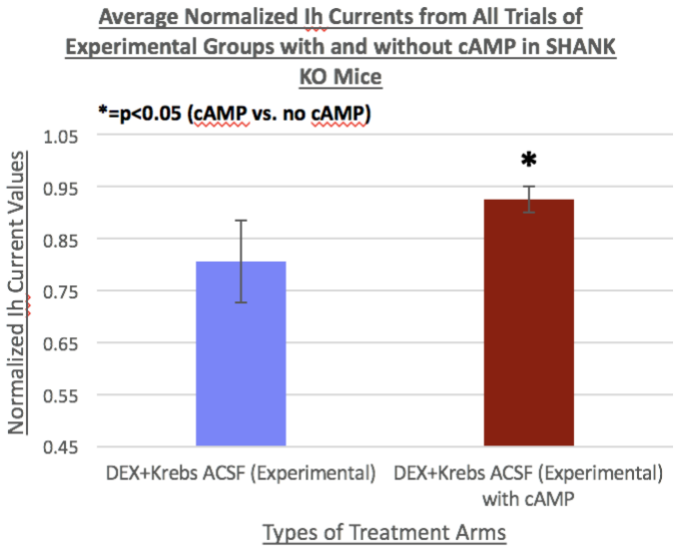

In SHANK 688 Knock-Out neurons (ASD model), the mean normalized Ih Current of the experimental group (DEX+ACSF) was still always lower than the control group (Krebs ACSF) both with and without cAMP. Raw data of the individual trials showed that the line of the normalized Ih current would "drop" in the presence of the experimental group. Without cAMP, all of the raw data trials showed that the reduction of the Ih current (caused by the 50nM DEX mixed solution) was statistically significant compared to Krebs ACSF (using two-tailed T-tests). Without cAMP, the p-value (measuring the means of Ih normalized currents) of the experimental group (DEX+ACSF) vs. the control group (Krebs ACSF) was 6.21×10^{-5} in SHANK 688 Knock-Out mice. Even with cAMP, the DEX+ACSF experimental group was still lower than the control group in SHANK 688 Knock-Out Neurons. Even in the SHANK 688 KO mice (ASD models), cAMP was significant in reducing the depression of the Ih Current caused by DEX. The p-value (measuring the means of Ih normalized currents) of the experimental group (DEX+ACSF) without cAMP vs. the experimental group (DEX+ACSF) with cAMP in SHANK KO mice was 0.01.

Part 3

Figure 7

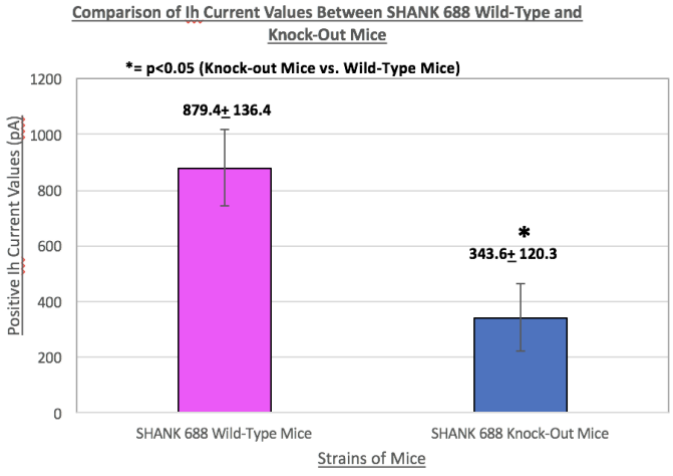

Figure 8

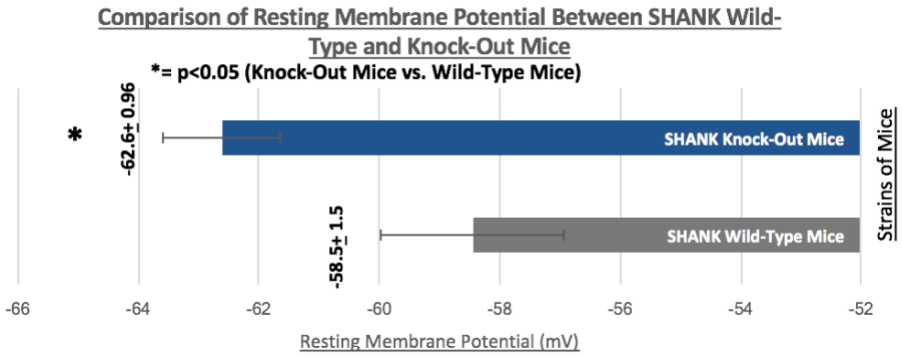

Figure 9

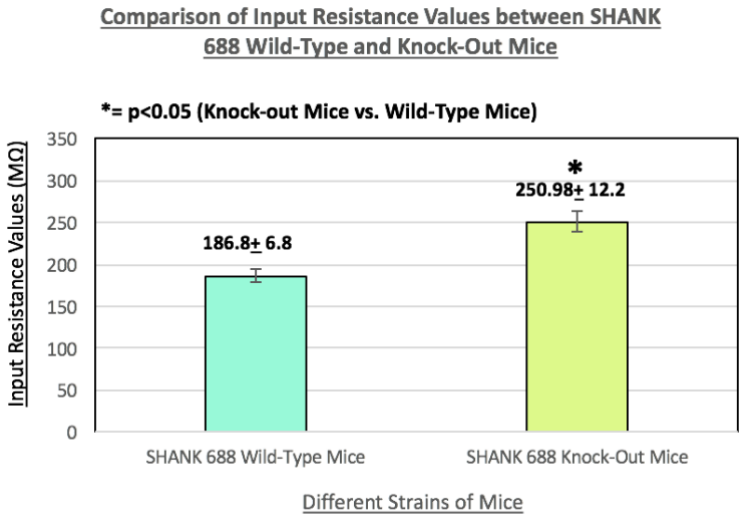

SHANK 688 Knock-Out neurons (ASD model) exhibited a statistically significant lower Ih current in pA (unnormalized and positive), compared to their respective SHANK 688 Wild-Type Neurons ($p = 2.63 \times 10^{-8}$). SHANK 688 Knock-Out Neurons (ASD model) showed a statistically significant lower RMP compared to their respective SHANK 688 Wild-Type Neurons ($p = 9.17 \times 10^{-8}$). SHANK 688 Knock-Out Neurons (ASD model) showed a statistically significant higher input resistance value compared to their respective SHANK 688 Wild-Type Neurons ($p = 2.17 \times 10^{-11}$).

Part 4

Figure 10

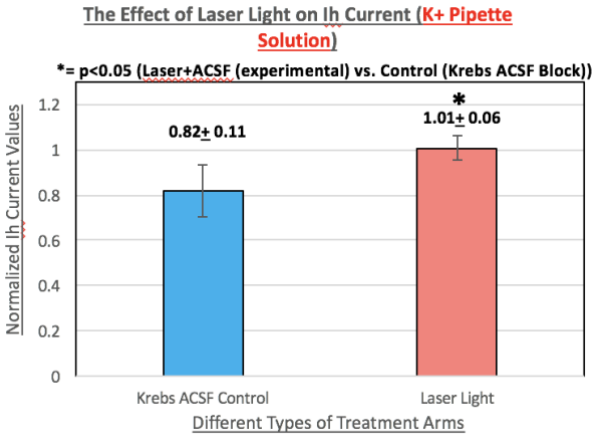

Figure 11

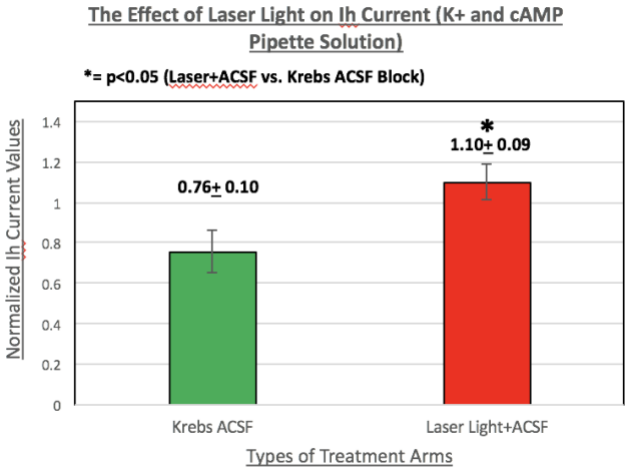

Figure 12

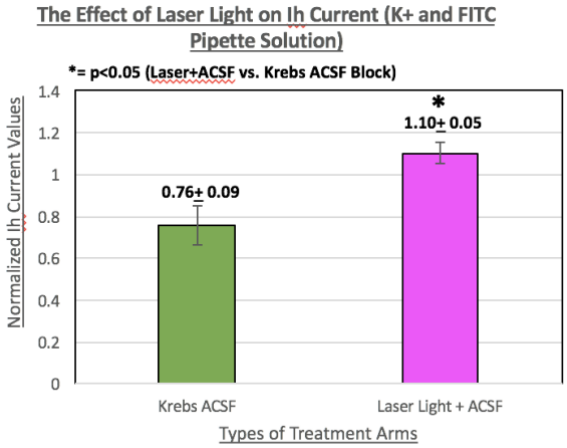

Figure 13

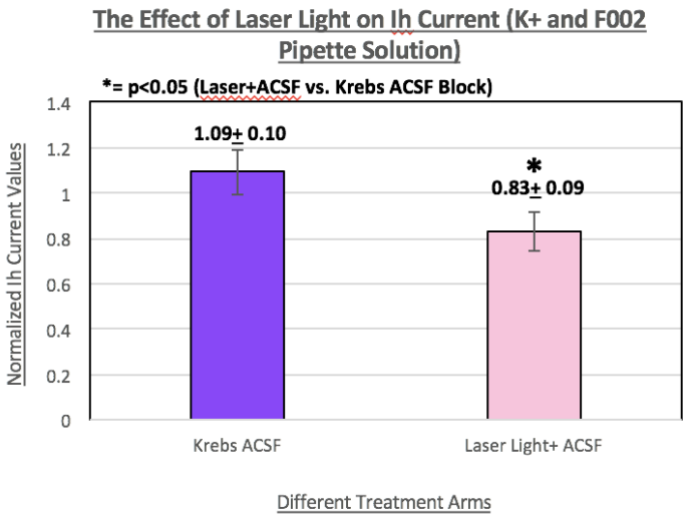

With the K+ pipette solution, the experimental group (laser+ACSF) significantly raised the Ih current. The p-value (measuring the means of Ih normalized currents) of the experimental group (Laser+ACSF) vs. the control group (Krebs ACSF) was 0.002. With the K+ and cAMP pipette solution, the laser+ACSF experimental group raised the Ih current even more than with the K+ pipette solution. The p-value (measuring the means of Ih normalized currents) of the experimental group (Laser+ACSF) vs. the control group (Krebs ACSF) was 2.07×10^{-7} with K+ and cAMP pipette solution. With the K+ and FITC pipette solution, the laser+ACSF experimental group raised the Ih current to about the same extent as with the K+ and cAMP pipette solution. The p-value (measuring the means of Ih normalized currents) of the experimental group (Laser+ACSF) vs. the control group (Krebs ACSF) was 2.02×10^{-6}. Surprisingly, with the K+ and F002 pipette solution, the laser+ACSF experimental group significantly lowered the Ih Current after the Krebs ACSF control treatment arm. The p-value (measuring the means of the Ih normalized currents) of the experimental group (laser+ACSF) vs. the control group (Krebs ACSF) was 7.88×10^{-6} .

F002 with and without Trolox C

F002 consists of an FITC compounded covalently bond to cAMP. FITC, a fluorescein, is a photosensitizer that reacts with O_2 in the air and light to form singlet oxygen (unstable and lowest excited state of O_2), leading to oxidation. Since cAMP may have bound to the HCN channel, the FITC compound (in F002) produce singlet Oxygen, which could be responsible for lowering the Ih current (novel finding). In order to test this prediction, the F002 + laser light treatment arm was tested in conjunction with an antioxidant called Trolox C.

Figure 11

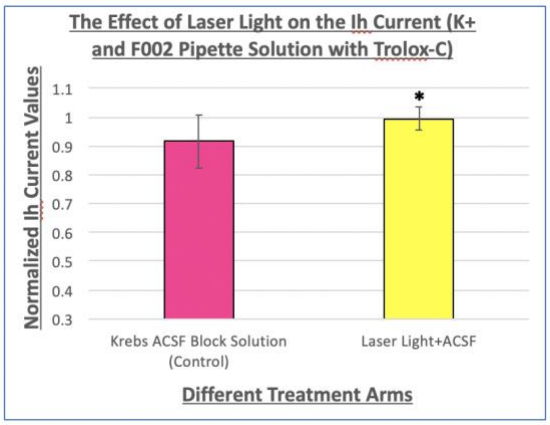

Figure 12

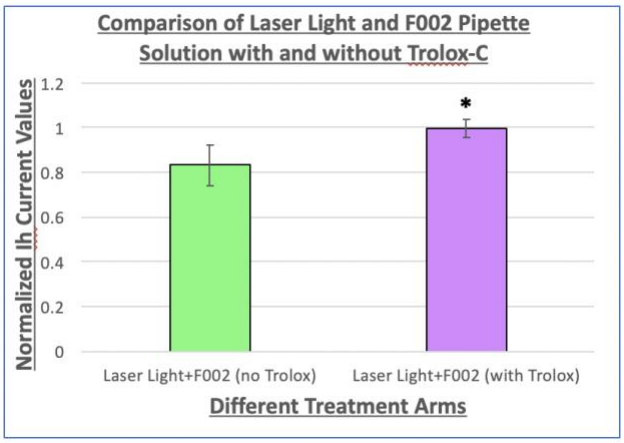

As shown in Figure 11, F002 in the presence of Trolox-C instead significantly raised the Ih current amplitude, rather than reduced it, when compared to the Krebs ACSF Block solution ($p = 0.013$). Trolox C helped reverse the effect of F002 on the Ih current, as the Ih current was significantly increased in the laser light + F002 (with Trolox) compared to the laser light without Trolox in Figure 12 ($p = 0.000132846$).

In-Silico Imaging: Computational Models of HCN2 Channel with cAMP

Using published x-ray crystallography data and x-ray crystallography data collected by my lab for the HCN channel, one of the largest program database (PDB) files was created for the HCN channel. The PDB file contained the entire structure of all 4 chains of the HCN Channel, (which were Chain A, Chain B, Chain C, and Chain D) as well as cAMP. It was later visualized on the Virtual Molecular Dynamics and CHARMM GUI membrane builder programs. Preliminary data concerning the atomic and molecular structures of the HCN channel were automatically calculated in the CHARMM GUI membrane-builder program.

Figure 13: In-silico image of the HCN2 Channel in the Virtual Molecular Dynamics Program.

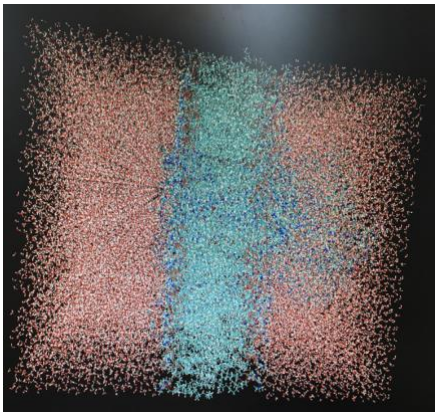

Figure 14: In-silico image of the HCN2 Channel in the CHAMM-GUI Membrane Builder program.

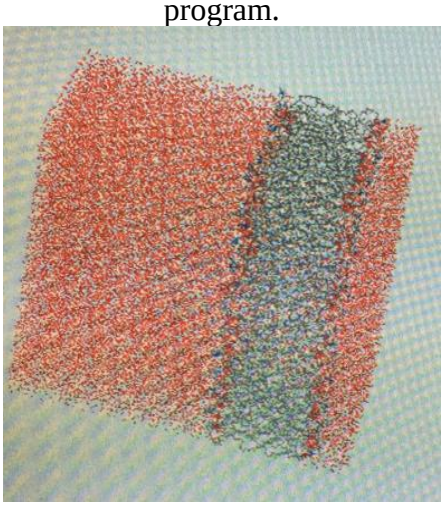

Figures 15 and 16: Membrane Builder Information of HCN2 Channel PDB File, Including System Size and Calculated Protein Cross-Sectional Area

Determined System Size:

# of Atoms	197757		
Crystal Type	TETRAGONAL		
System Size	A	119.268153	Dimension along the A (X) axis
	B	119.268153	Dimension along the B (Y) axis
	C	153.438	Dimension along the C (Z) axis
Crystal Angle	Alpha	90.0	Angle between the axis B and C
	Beta	90.0	Angle between the axis A and C
	Gamma	90.0	Angle between the axis A and B
Lipid			
# of Lipids	on Top	120	
	on Bottom	120	
# of Water	42863		
# of POT Ion	122		
# of CLA Ion	138		
Z Center	0.0		Center of the system along the Z axis

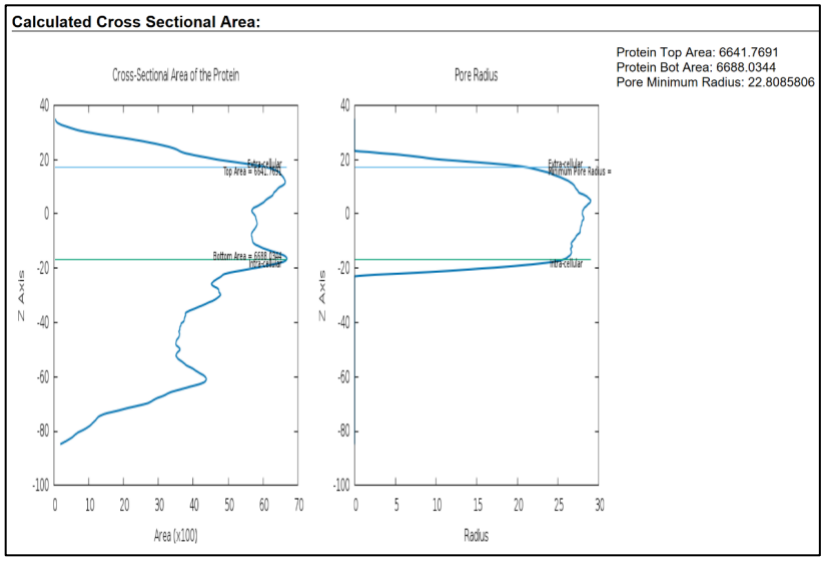

Discussions and Conclusions

The purpose of this experiment was to test the effect of the DEX and laser light pulses (with various compounds) on the Ih current of the HCN Channel in SHANK WT and KO neurons. The majority of the hypotheses were accepted. Overall, this study found several major, novel findings.

In summary, this study proves that DEX inhibits the Ih current of HCN2 channels in both SHANK 688 Wild-Type and SHANK 688 Knock-Out thalamus neurons. In addition, it also proves that cAMP minimizes the reduction of the Ih current caused by DEX in both SHANK 688 Wild-Type and SHANK 688 Knock-Out mice.

This study also is successful in finding potential novel electrophysiological biomarkers about Autism Spectrum Disorder, as SHANK 688 Knock-Out Mice showed lower positive Ih current values, lower resting membrane potential values, and a higher input resistance, which can lead to decreased neuronal transmissions and dendritic integration. Additionally, laser light stimulation in general seemed to significantly improve the Ih current (with the K+, K+ and cAMP, and K+ and FITC pipette solution).

One initial unexpected result (incorrect hypothesis) was that the effect of laser light+ACSF with the F002 pipette solution significantly lowered the Ih current. However, Fluorescein FITC has the ability to react with O_2 in the air and light to form singlet oxygen (unstable and lowest excited state of O_2). Singlet oxygen is considered as part of the reactive oxygen species (ROS). Studies have previously shown that increase levels of ROS may result in significant damage to cell structures, cumulatively known as oxidative stress. It was subsequently predicted that oxidative stress from the single oxygen being produced in the F002 compound lowered the Ih current. This prediction was later validated, as when the laser light + F002 compound was studied in conjunction with the antioxidant Trolox C, the Ih current was significantly higher compared to the control Krebs ACSF block solution, as well as the laser light + F002 without Trolox C. Therefore, another novel finding of this study shows the importance that oxidative stress can also have damaging effects on our body's natural pacemaker electrical currents, like the Ih current. However, antioxidants like Trolox C can be crucial when oxidative stress may deter one's Ih current.

The findings of Part 3 of this study were correlated to a Stanford study, which showed

that Shank 3 KO mice (lacking exon 3) had a significantly lower Ih current in their hippocampus neurons (Yi et al., 2016). This novel finding could provide novel cellular and electrophysiological biomarkers that may play an impact with the occurrence of ASD. However, laser therapy (as well as cAMP and also FITC) may be used as novel treatments for the Ih current suppression in patients with Autism Spectrum Disorder.

The results of this study are important as the lowering of the Ih current can have detrimental effects, since it is crucial in many vital functions. For example, it helps generate spontaneous pacemaker activity in the heart, central nervous system, and seven other organs. It also controls the resting potential (of a cell), membrane resistance and dendritic integration, and the regulation of synaptic transmission. This study shows that one would have to take caution before giving any sedatives to patients that already have a lowered Ih current (like ASD patients), or cautious of oxidative stress on electrical currents in the body. However, this experiment builds upon novel research displaying connections between Ih electrical currents and neuropsychiatric disorders like Autism Spectrum Disorders. Future studies could correlate natural electrical currents within the brain to other neuropsychiatric disorders (like schizophrenia) or even neurodegenerative disorders (like Alzheimer's Disease).

One limitation of this study was not incorporating the Krebs ACSF Wash group in my statistical analyses. One future study would be to compare the DEX+ACSF experimental group with the Krebs ACSF wash group. Another future study would be to test the differences between SHANK688$_{\Delta 13–16}$ Wild-Type and SHANK688$_{\Delta 13–16}$ Heterozygous thalamus neurons. A third future study could also build upon preliminary in-silico PDB data displaying the images of the HCN Channel with cAMP on the Virtual Molecular Dynamics Program. For example, the exact binding sites within the atomic structure patterns of the HCN Channel and cAMP can be found, which can be useful for delivering therapies for patients with a lower or deterred Ih current.

Bonus Extension to Research Project: Current Study Discovering Structural Differences in the Brain Between Healthy and ASD Patients

Transcranial Magnetic Stimulation is noninvasive procedure that uses magnetic fields to stimulate nerve cells in the brain to improve symptoms typically of depression. However, the effects of TMS on Parkinson's, schizophrenia, or/and other neuropsychiatric diseases has become of interest.

Transcranial magnetic stimulation (TMS), use probes placed on or near the scalp. The distance between the scalp and the brain is a key variable for these techniques because optical, electrical and magnetic signals are attenuated by distance. However, little is known about how scalp-brain distance differs between different cortical regions in children or how it changes with development, as well as seeing structural differences in patients with neuropsychiatric diseases (particularly Autism).

In order to conduct this bonus study, MRI data from the patient of interest. Using Linux-based software, PDB files were made and combined subsequently to make one entire PDB file of the brain model of interest. Using the computational constructed brain model, brain-scalp distances and volumes were calculated with the "volBrain" website and analyzed between patients that were healthy and patients that had autism spectrum disorders. The brain-scalp distance was calculated in the M1 area and the dorsolateral prefrontal cortex (DLPFC) of the brain.

Figure: MRI Image of Brain of Patient with Autism

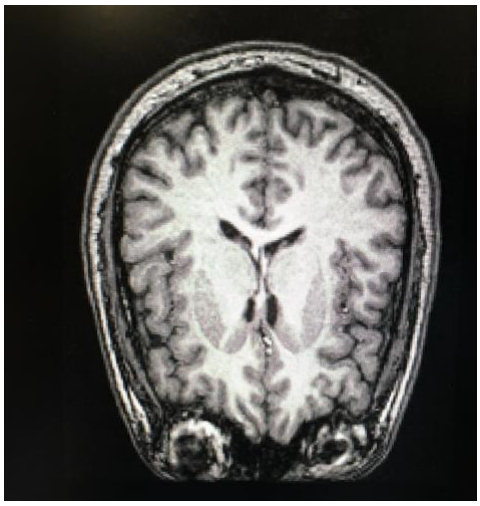

Figures: Constructed Brain Models from MRI Data of Healthy Patients

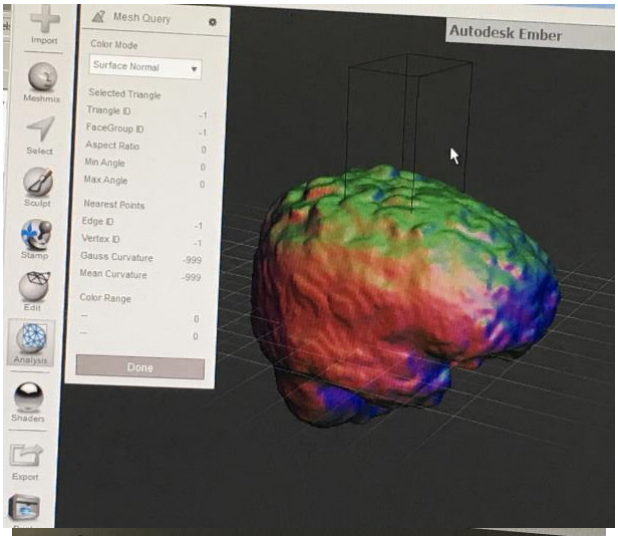

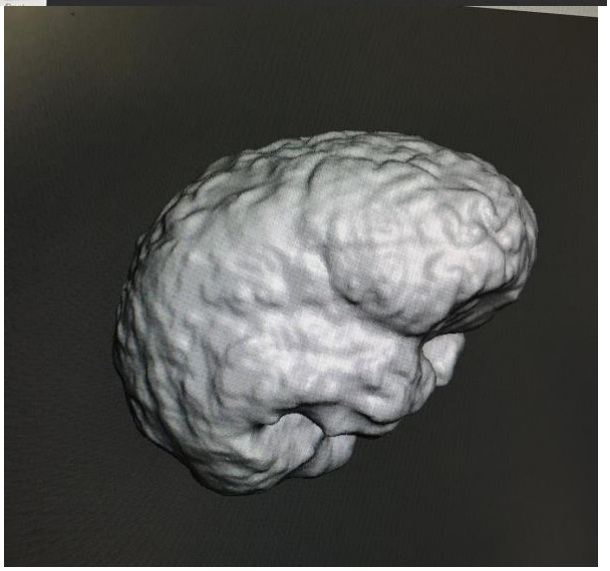

<u>Results of Brain Volume and Scalp-Distances Data Between Young Healthy, Old Healthy and Autism Patients</u>

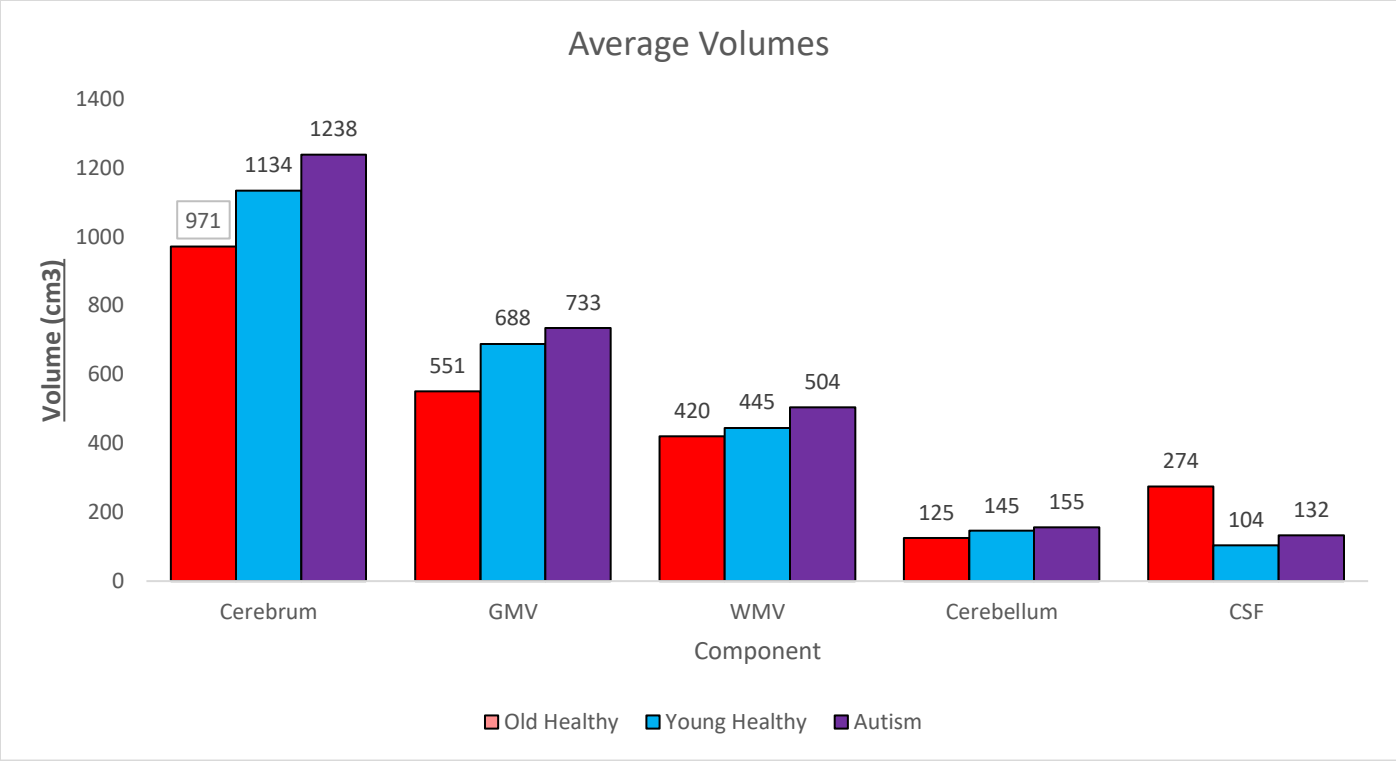

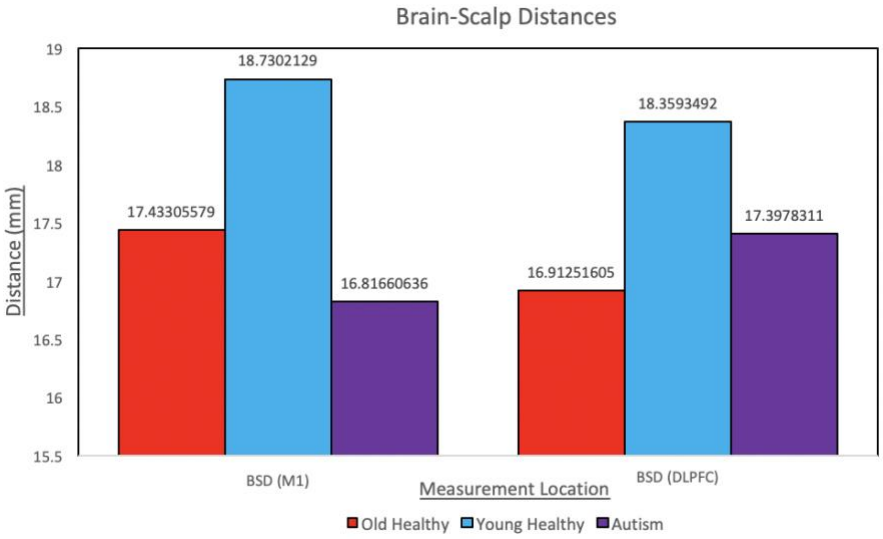

Initial findings show that Autism patients tend to have a higher cerebrum, gray matter, white matter, and cerebellum volume. Additionally, Autism patients have a lower brain to scalp distance in the M1 region of the brain, as well as have a higher brain to scalp distance in the DLPFC region compared to old healthy patients. Determining the brain to scalp distances are essential for determining to use TMS as a treatment for patients with autism spectrum disorders. Additionally, it would further the field of neuroscience when determining structural brain differences (such as in certain regions of the brain), which could ultimately be utilized as biomarkers for certain neuropsychiatric diseases. The differences in volumes in certain regions of the brain could explain the behavior of patients with certain neuropsychiatric diseases (like ASD).

Appendix A

This is an example of the electrophysiological pattern of the Ih Current in one trial (derived from the effect of DEX without cAMP on the Ih current in SHANK Wild Type Mice).

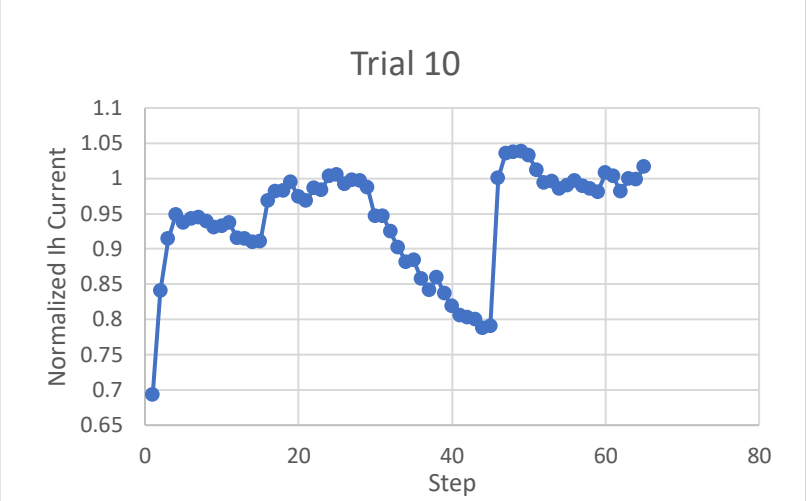

In addition, there is an example of what the raw data for the previous trial

Resting Membrane Potential		Imacro-Iinst			offset:116.10
-58.2	Steps	**Actual Ih current values**	Normalized Ih Current Values	Voltage	Voltage-Offset
171221_005.2 Ih[1-65].abf	1	-709.77	0.69	17.18	-99.02
171221_005.2 Ih[1-65].abf	2	-860.65	0.84	17.19	-99.01
171221_005.2 Ih[1-65].abf	3	-936.27	0.91	17.17	-99.03
171221_005.2 Ih[1-65].abf	4	-971.31	0.95	17.18	-99.02
171221_005.2 Ih[1-65].abf	5	-959.67	0.94	17.19	-99.01
171221_005.2 Ih[1-65].abf	6	-965.92	0.94	17.18	-99.02
171221_005.2 Ih[1-65].abf	7	-967.49	0.94	17.19	-99.01
171221_005.2 Ih[1-65].abf	8	-962.19	0.94	17.18	-99.02
171221_005.2 Ih[1-65].abf	9	-953.10	0.93	17.17	-99.03
171221_005.2 Ih[1-65].abf	10	-955.27	0.93	17.19	-99.01
171221_005.2 Ih[1-65].abf	11	-959.58	0.94	17.19	-99.01

171221_005.2 Ih[1-65].abf	12	-937.99	0.92	17.20	-99.00
171221_005.2 Ih[1-65].abf	13	-936.48	0.91	17.18	-99.02
171221_005.2 Ih[1-65].abf	14	-931.65	0.91	17.18	-99.02
171221_005.2 Ih[1-65].abf	15	-932.64	0.91	17.21	-98.99
171221_005.2 Ih[1-65].abf	16	-991.76	0.97	17.19	-99.01
171221_005.2 Ih[1-65].abf	17	-1005.73	0.98	17.20	-99.00
171221_005.2 Ih[1-65].abf	18	-1006.48	0.98	17.19	-99.01
171221_005.2 Ih[1-65].abf	19	-1018.59	0.99	17.17	-99.03
171221_005.2 Ih[1-65].abf	20	-998.01	0.97	17.18	-99.02
171221_005.2 Ih[1-65].abf	21	-991.69	0.97	17.18	-99.02
171221_005.2 Ih[1-65].abf	22	-1010.15	0.99	17.19	-99.01
171221_005.2 Ih[1-65].abf	23	-1007.61	0.98	17.20	-99.00
171221_005.2 Ih[1-65].abf	24	-1028.21	1.00	17.18	-99.02
171221_005.2 Ih[1-65].abf	25	-1029.31	1.00	17.18	-99.02
171221_005.2 Ih[1-65].abf	26	-1016.40	0.99	17.19	-99.01
171221_005.2 Ih[1-65].abf	27	-1021.64	1.00	17.18	-99.02
171221_005.2 Ih[1-65].abf	28	-1021.05	1.00	17.19	-99.01
171221_005.2 Ih[1-65].abf	29	-1011.11	0.99	17.18	-99.02
171221_005.2 Ih[1-65].abf	30	-969.25	0.95	17.18	-99.02
171221_005.2 Ih[1-65].abf	31	-969.80	0.95	17.17	-99.03
171221_005.2 Ih[1-65].abf	32	-947.21	0.92	17.19	-99.01
171221_005.2 Ih[1-65].abf	33	-923.72	0.90	17.19	-99.01
171221_005.2 Ih[1-65].abf	34	-903.18	0.88	17.20	-99.00
171221_005.2 Ih[1-65].abf	35	-905.60	0.88	17.19	-99.01

171221_005.2 Ih[1-65].abf	36	-878.32	0.86	17.18	-99.02
171221_005.2 Ih[1-65].abf	37	-861.87	0.84	17.21	-98.99
171221_005.2 Ih[1-65].abf	38	-880.86	0.86	17.20	-99.00
171221_005.2 Ih[1-65].abf	39	-857.06	0.84	17.18	-99.02
171221_005.2 Ih[1-65].abf	40	-838.33	0.82	17.18	-99.02
171221_005.2 Ih[1-65].abf	41	-825.31	0.81	17.18	-99.02
171221_005.2 Ih[1-65].abf	42	-822.67	0.80	17.18	-99.02
171221_005.2 Ih[1-65].abf	43	-819.73	0.80	17.17	-99.03
171221_005.2 Ih[1-65].abf	44	-806.52	0.79	17.18	-99.02
171221_005.2 Ih[1-65].abf	45	-809.99	0.79	17.17	-99.03
171221_005.2 Ih[1-65].abf	46	-808.93	0.79	17.17	-99.03
171221_005.2 Ih[1-65].abf	47	-836.95	0.82	17.16	-99.04
171221_005.2 Ih[1-65].abf	48	-838.33	0.82	17.17	-99.03
171221_005.2 Ih[1-65].abf	49	-839.32	0.82	17.18	-99.02
171221_005.2 Ih[1-65].abf	50	-834.47	0.81	17.18	-99.02
171221_005.2 Ih[1-65].abf	51	-818.04	0.80	17.17	-99.03
171221_005.2 Ih[1-65].abf	52	-803.44	0.78	17.18	-99.02
171221_005.2 Ih[1-65].abf	53	-804.58	0.79	17.17	-99.03
171221_005.2 Ih[1-65].abf	54	-796.37	0.78	17.16	-99.04
171221_005.2 Ih[1-65].abf	55	-800.15	0.78	17.16	-99.04
171221_005.2 Ih[1-65].abf	56	-805.28	0.79	17.17	-99.03
171221_005.2 Ih[1-65].abf	57	-799.66	0.78	17.18	-99.02
171221_005.2 Ih[1-65].abf	58	-796.47	0.78	17.18	-99.02
171221_005.2 Ih[1-65].abf	59	-792.71	0.77	17.18	-99.02

171221_005.2 Ih[1-65].abf	60	-814.36	0.79	17.17	-99.03
171221_005.2 Ih[1-65].abf	61	-810.88	0.79	17.19	-99.01
171221_005.2 Ih[1-65].abf	62	-792.98	0.77	17.19	-99.01
171221_005.2 Ih[1-65].abf	63	-807.75	0.79	17.20	-99.00
171221_005.2 Ih[1-65].abf	64	-806.79	0.79	17.17	-99.03
171221_005.2 Ih[1-65].abf	65	-821.35	0.80	17.18	-99.02

F-Test Two-Sample for Variances		
	Variable 1 (Control)	*Variable 2 (DEX treatment)*
Mean	0.935215051	0.887584137
Variance	0.003993652	0.005335157
Observations	24	19
df	23	18
F	0.748553892	
P(F<=f) two-tail	0.506883288	
t-Test: Two-Sample Assuming Equal Variances		
	Variable 1	*Variable 2*
Mean	0.935215051	0.887584137
Variance	0.003993652	0.005335157
Observations	24	19
Pooled Variance	0.004582605	
Hypothesized Mean Difference	0	
df	41	
t Stat	2.2912943	
P(T<=t) one-tail	0.013578335	
t Critical one-tail	1.682878002	
P(T<=t) two-tail	0.027156671	
t Critical two-tail	2.01954097	

Appendix B

This section provides more information about the Ih current in various experiments with each trial.

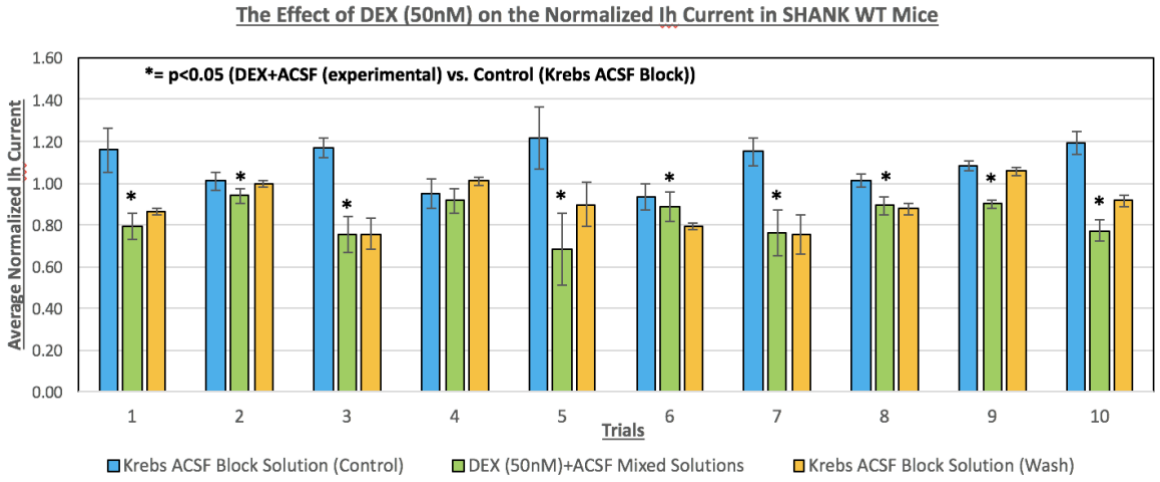

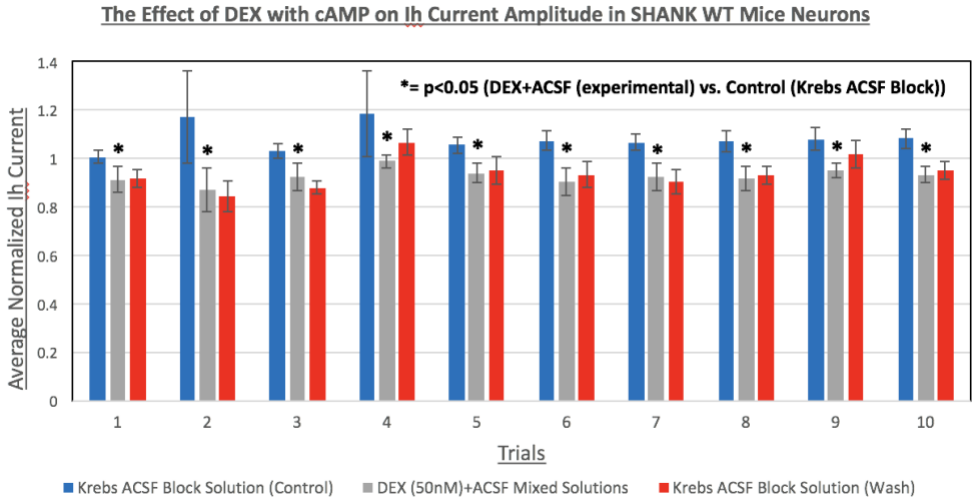

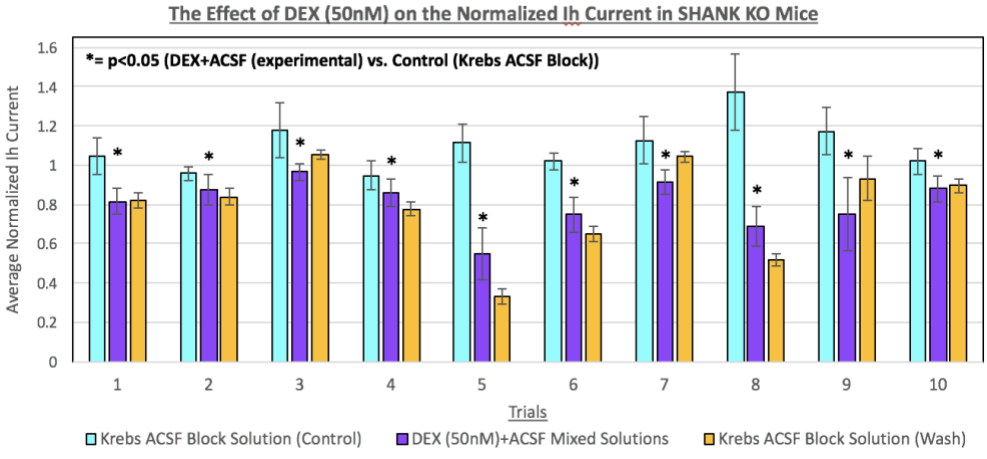

The Effect of DEX with cAMP on Ih Current Amplitude in SHANK KO Mice Neurons

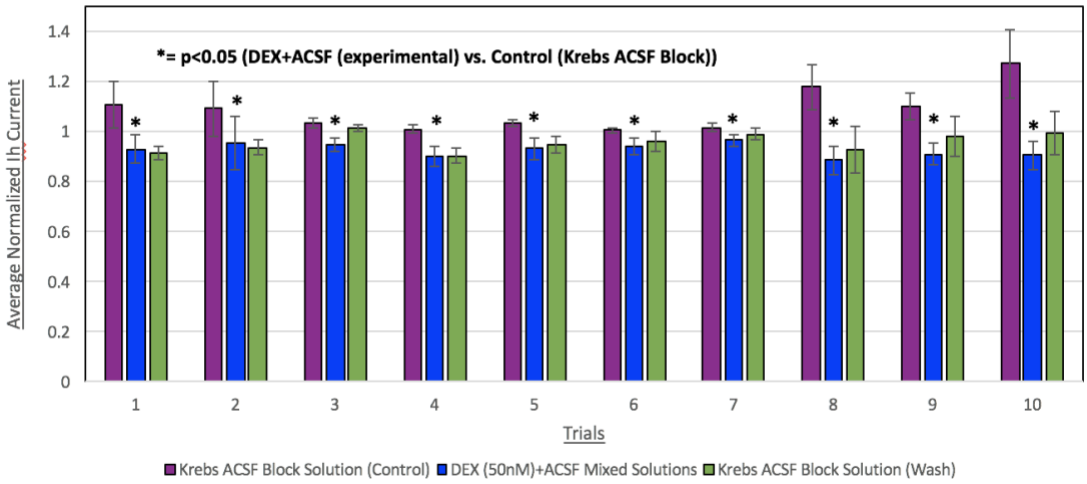

The Effect of Laser Light on the Ih Current (K+ Pipette Solution)

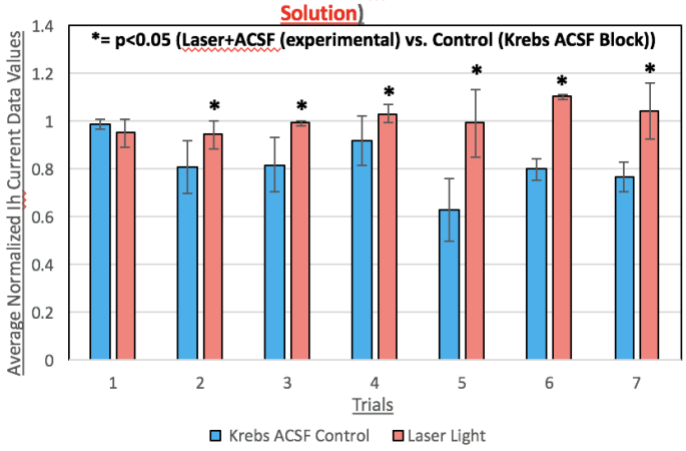

The Effect of Laser Light on Ih Current (K+ and cAMP Pipette Solution)

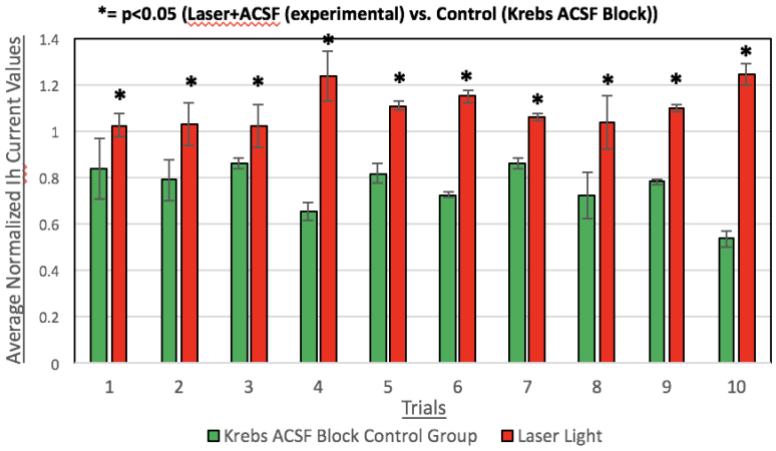

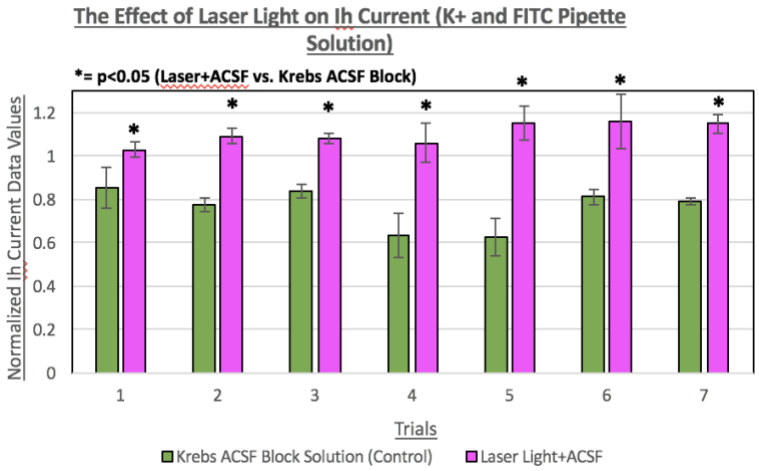
The Effect of Laser Light on Ih Current (K+ and FITC Pipette Solution)
*= p<0.05 (Laser+ACSF vs. Krebs ACSF Block)
Normalized Ih Current Data Values
0
0.2
0.4
0.6
0.8
1
1.2
1
2
3
4
5
6
7
Trials
Krebs ACSF Block Solution (Control)
Laser Light+ACSF

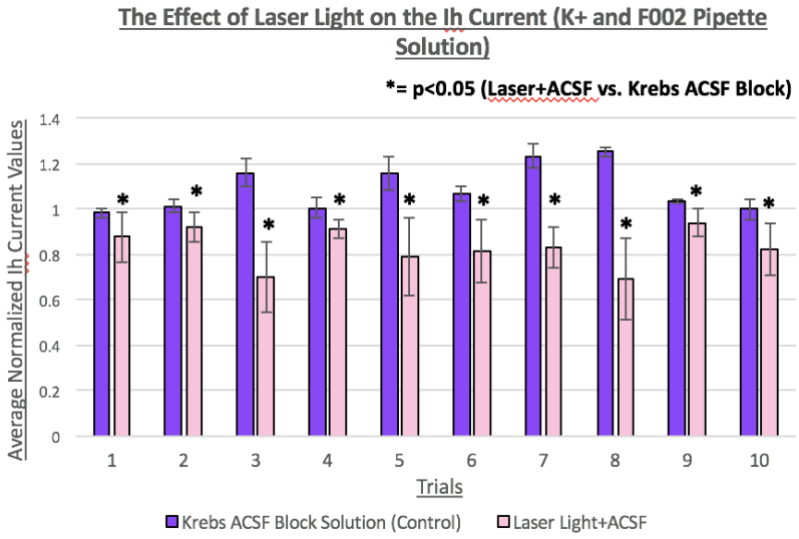
The Effect of Laser Light on the Ih Current (K+ and F002 Pipette Solution)
*= p<0.05 (Laser+ACSF vs. Krebs ACSF Block)
Average Normalized Ih Current Values
0
0.2
0.4
0.6
0.8
1
1.2
1.4
1
2
3
4
5
6
7
8
9
10
Trials
Krebs ACSF Block Solution (Control)
Laser Light+ACSF

Appendix C

This section includes more information about the mean and standard deviation from the different aspects of the project.

Table 1: The Effect of DEX (50nM) on the Normalized Ih Current in SHANK WT Mice

Trial Number	1	2	3	4	5	6	7	8	9	10
Krebs ACSF Block Solution (Control)	1.16± 0.11	1.01± 0.04	1.17± 0.05	0.95± 0.07	1.22± 0.15	0.94± 0.06	1.15± 0.06	1.01± 0.03	1.08± 0.02	1.19± 0.06
DEX (50nM)+ACSF Mixed Solution	0.80± 0.06	0.94± 0.04	0.76± 0.08	0.91± 0.06	0.69± 0.17	0.89 ± 0.07	0.76 ± 0.11	0.89± 0.04	0.90± 0.02	0.77± 0.05
KREBS ACSF Block Solution (Wash)	0.87± 0.02	1.00± 0.02	0.76± 0.08	1.01± 0.02	0.90± 0.10	0.79± 0.01	0.75± 0.09	0.88± 0.03	1.06± 0.02	0.92± 0.03

Table 2: The Effect of DEX (50nM) on the Normalized Ih Current in SHANK KO Mice

Trial number	1	2	3	4	5	6	7	8	9	10
Krebs ACSF Block Solution	1.07± 0.10	0.96± 0.38	1.18± 0.14	0.95± 0.07	1.11± 0.1	1.02± 0.04	1.13± 0.12	1.37± 0.19	1.17± 0.12	1.02± 0.07
Dex(50nM) + ACSF Mixed Solution	0.93± 0.05	0.87± 0.07	0.97± 0.04	0.86± 0.06	0.55± 0.13	0.75± 0.09	0.92± 0.06	0.69± 0.1	0.75± 0.19	0.94± 0.04
Krebs ACSF Block Solution (Wash)	0.86± 0.03	0.84± 0.04	1.05± 0.02	0.78± 0.04	0.33 ± 0.04	0.65± 0.04	1.04± 0.02	0.52± 0.03	0.93± 0.03	1.00± 0.03

Table 3: Comparison of Positive Ih Current Values (pA) Between SHANK WT and KO Mice

SHANK WT Mice	879.35 ± 136.39
SHANK KO Mice	343.6 ± 120.38

Table 4: The Effect of DEX + cAMP on Ih Current Amplitude in SHANK KOMice Neurons

Trial Number	1	2	3	4	5	6	7	8	9	10
Krebs ACSF Block Solution (Control)	1.14± 0.09	1.09± 0.11	1.03± 0.02	1.01± 0.02	1.03± 0.02	1.0± 0.01	1.01± 0.02	1.18± 0.09	1.1± 0.05	1.28± 0.14
DEX (50 Nm) + ACSF Mixed Solutions	0.93± 0.05	0.95± 0.10	0.94± 0.03	0.90± 0.04	0.93± 0.04	0.94± 0.03	0.96± 0.02	0.88± 0.06	0.91± 0.05	0.81± 0.09
Krebs ACSF Block Solution (Wash)	0.91± 0.03	0.93± 0.03	1.01± 0.01	0.9± 0.03	0.95± 0.03	0.96± 0.04	0.99± 0.02	0.93± 0.09	0.98± 0.08	0.96± 0.13

Table 5: The Effect of DEX with cAMP on Ih Current Amplitude in SHANK WT Mice Neurons

Trial Number	1	2	3	4	5	6	7	8	9	10
Krebs ACSF Block Solution (Control)	1.01± 0.03	1.17± 0.20	1.03± 0.03	1.18± 0.18	1.06± 0.35	1.07± 0.04	1.07± 0.04	1.07± 0.04	1.08±0. 04	1.08± 0.04
DEX (50nM)+ACSF Mixed Solution	0.91± 0.05	0.87± 0.09	0.92± 0.06	0.99± 0.03	0.94± 0.04	0.91 ± 0.06	0.92 ± 0.06	0.92± 0.05	0.95± 0.03	0.93± 0.03
KREBS ACSF Block Solution (Wash)	0.91± 0.04	0.84± 0.06	0.88± 0.03	1.07± 0.05	0.95± 0.06	0.93± 0.06	0.90± 0.05	0.93± 0.04	1.01± 0.06	0.95± 0.04

Table 6: The Effect of Laser Light on the Ih Current (K+ Pipette Solution)

Trials	1	2	3	4	5	6	7
Krebs ACSF (Control)	0.99± 0.01	0.81± 0.11	0.82± 0.11	0.92± 0.10	0.63± 0.12	0.80± 0.05	0.77± 0.06
Laser Light+ACSF	0.95± 0.06	0.94± 0.06	0.99± 0.01	1.03± 0.04	0.99± 0.14	1.10± 0.01	1.05± 0.12

Table 7: The Effect of Laser Light on the Ih Current (K+ and cAMP Pipette Solution)

Trials	1	2	3	4	5	6	7	8	9	10
Krebs ACSF (Control)	0.84± 0.13	0.79± 0.09	0.86± 0.02	0.65± 0.04	0.81± 0.04	0.72± 0.01	0.86± 0.02	0.72± 0.10	0.78± 0.01	0.53± 0.04
Laser Light Pulse+ACSF	1.02± 0.05	1.03± 0.09	1.02± 0.09	1.24± 0.11	1.11± 0.02	1.15± 0.03	1.06± 0.01	1.04± 0.12	1.10± 0.01	1.24± 0.05

Table 8: The Effect of Laser Light on the Ih Current (K+ and FITC Pipette Solution)

Trials	1	2	3	4	5	6	7
Krebs ACSF (Control)	0.85± 0.09	0.78± 0.03	0.84± 0.03	0.63± 0.10	0.62± 0.09	0.81± 0.03	0.79± 0.01
Laser Light+ACSF	1.03± 0.03	1.09± 0.03	1.08± 0.02	1.06± 0.09	1.15± 0.08	1.16± 0.12	1.15± 0.04

Table 9: The Effect of Laser Light on the Ih Current (K+ and F002 Pipette Solution)

Trials	1	2	3	4	5	6	7	8	9	10
Krebs ACSF (Control)	0.98± 0.02	1.01± 0.03	1.16± 0.06	1.01± 0.05	1.16± 0.08	1.07± 0.03	1.23± 0.05	1.25± 0.02	1.03± 0.01	1.00± 0.04
Laser Light+ACSF	0.88± 0.11	0.92± 0.07	0.70± 0.16	0.91± 0.04	0.79± 0.17	0.82± 0.14	0.83± 0.09	0.69± 0.18	0.94± 0.06	0.83± 0.11

Appendix D

Picture 1: Experimental set up of patch-clamp technique, depicting the 1000X microscope and the containers of the Krebs ACSF (to maintain cell viability) Block and Wash solutions, as well as DEX.

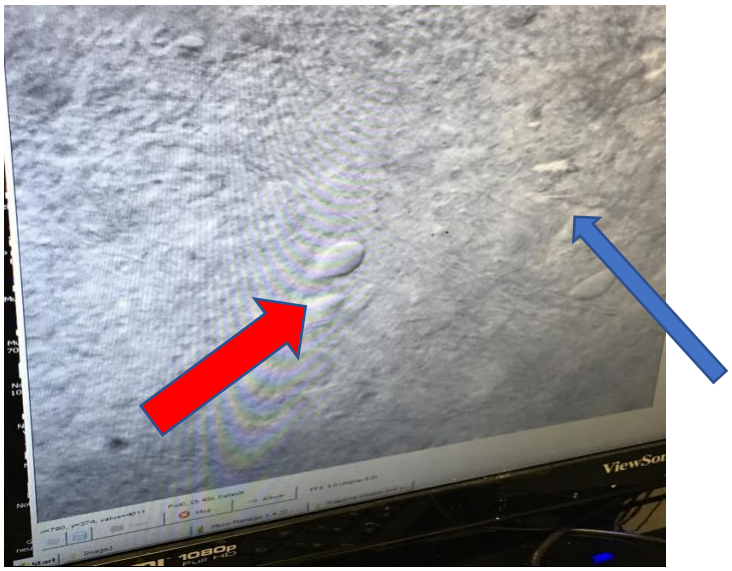

Picture 2: Microscopic view of mice thalamus neurons (shown by the red arrow) with the micropipette (as shown by the long blue arrow).

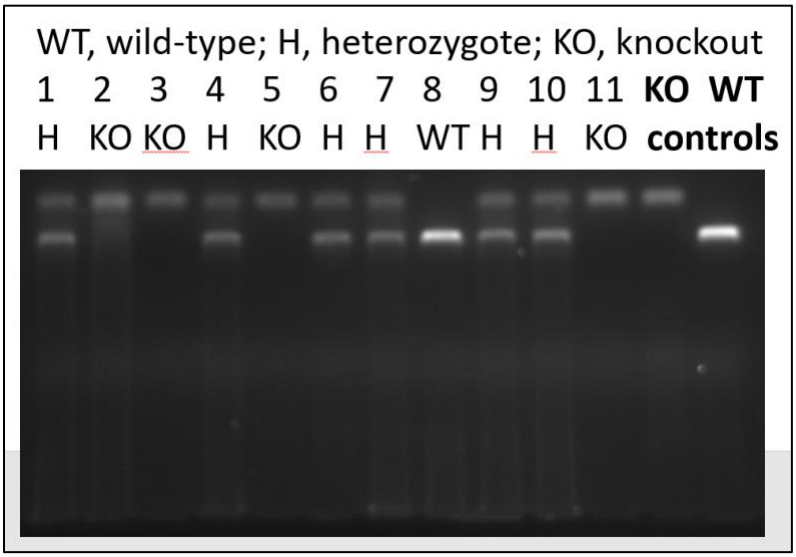

Picture 3: Genotyping mouse tails as either SHANK 688 Knock-Out (KO), Heterozygous (H), or Wild-Type (WT)

Appendix E

Sample (first page) of the PDB file of the HCN Channel (consisting entire of 631 pages)

```
CRYST1    0.000    0.000    0.000  90.00  90.00  90.00 P 1           1
ATOM      1  N   LEU A   1       1.293  55.510 -20.321  1.00 21.99
N
ATOM      2  CA  LEU A   1       0.208  55.491 -19.315  1.00 21.99
C
ATOM      3  CB  LEU A   1      -0.369  56.905 -19.127  1.00 21.99
C
ATOM      4  CG  LEU A   1       0.648  57.906 -18.545  1.00 21.99
C
ATOM      5  CD1 LEU A   1       0.030  59.303 -18.373  1.00 21.99
C
ATOM      6  CD2 LEU A   1       1.280  57.368 -17.252  1.00 21.99
C
ATOM      7  C   LEU A   1      -0.895  54.577 -19.739  1.00 21.99
C
ATOM      8  O   LEU A   1      -0.816  53.363 -19.560  1.00 21.99
O
ATOM      9  N   GLN A   2      -1.964  55.163 -20.306  1.00 72.04
N
ATOM     10  CA  GLN A   2      -3.121  54.439 -20.746  1.00 72.04
C
ATOM     11  CB  GLN A   2      -4.239  55.388 -21.210  1.00 72.04
C
ATOM     12  CG  GLN A   2      -3.849  56.246 -22.414  1.00 72.04
C
ATOM     13  CD  GLN A   2      -4.939  57.288 -22.619  1.00 72.04
C
ATOM     14  OE1 GLN A   2      -6.122  57.015 -22.422  1.00 72.04
O
ATOM     15  NE2 GLN A   2      -4.532  58.524 -23.012  1.00 72.04
N
ATOM     16  C   GLN A   2      -2.754  53.543 -21.887  1.00 72.04
C
ATOM     17  O   GLN A   2      -3.237  52.413 -21.973  1.00 72.04
O
ATOM     18  N   ARG A   3      -1.876  54.024 -22.786  1.00129.52
N
ATOM     19  CA  ARG A   3      -1.501  53.286 -23.961  1.00129.52
C
ATOM     20  CB  ARG A   3      -0.435  54.023 -24.787  1.00129.52
C
ATOM     21  CG  ARG A   3      -0.012  53.303 -26.070  1.00129.52
C
ATOM     22  CD  ARG A   3       1.251  53.895 -26.704  1.00129.52
C
ATOM     23  NE  ARG A   3       2.296  52.833 -26.748  1.00129.52
N
ATOM     24  CZ  ARG A   3       2.402  52.050 -27.862  1.00129.52
```

【評語】080020

Sedatives are medicines taken for their calming and soporific effects. Dexmedetomidine (DEX) has sedative effects and is known to be an alpha2 adrenoceptor (a G protein-coupled receptor) agonist. The HCN (hyperpolarization-activated cyclic nucleotide-gated) channels are a type of pore-loop cation channels (Robinson, 2002). The cation current that runs through HCN channels is called the Ih current (Benarroch, 2013). In their project, they studied EX's effect on the Ih current.

Strong points:

The research question for this project was: "Can Dexmedetomidine lower the Ih Current Amplitude of the HCN Channel in Mus Musculus?" DEX's effect on the Ih current has never been studied, so there is novelty, although somewhat related to Chen's research, who discovered that DEX inhibits both sodium and calcium currents. This topic is important to study because if DEX does indeed lower the Ih current, it will lead to behavioral defects and affect the excitability of neurons in the human body. It is commendable for your hard work on this project, and lots of data were generated from this study.

Weakness:

The results only contain a Fig. that seems too simple. More studies as they propose can be also studied. They mentioned an outlier in Trial 5 (Appendix B) that might have been caused if the DEX concentration was not mixed too well or if it had been a little more dilute. However, from Fig. 1, trial 4 shows

similar trends to that of trial 5. Is trial 4 also an outlier? In appendix B, there are raw data for only six trials, but in Fig. 1, there are 10 trials. Did they miss somethings?

Research Comments:

1. The writing of this report was in the logical progression, however, proper scientific references are missing in the report. It is recommended to define RMP shown on page 9. What is RMP?
2. The unit of Ih current values is suggested to provide in Y-axis of all your figures. It is recommended to include the treatment of antioxidant Trolox C in Overview of Science Project on page 5. Figures 11 and 12 on page 12 are duplicated and shall be changed to 14 and 15, and the rests of all figures shall be changed accordingly.